第 26 卷第 2 期 无 机 化 学 学 报 Vol.26 No.2
2010 年 2 月 CHINESE JOURNAL OF INORGANIC CHEMISTRY 274-278

不同形貌 YF_3 微米晶的水热合成及 YF_3:Eu^{3+}荧光性质

王 森 孙同明 石玉军*
(南通大学化学化工学院,南通 226007)

摘要:水热条件下,$Y(NO_3)_3\cdot 6H_2O$ 分别与 K_2SiF_6、KPF_6 反应得到了不同形貌的 YF_3(八面体及椭球形)。以 X 射线光电子能谱(XPS)检测了产物的化学组成,表明产物中只含有 Y 和 F。X 射线衍射(XRD)结果表明所得的产物均为正交晶系。扫描电子显微镜(SEM)和透射电子显微镜(TEM)对产物的表征结果指明八面体形 YF_3 棱长为 200 nm,而椭球形 YF_3 是由小的纳米块自组装而成。还研究了 Eu^{3+}掺杂后 YF_3 的荧光性质,并提出了可能的形成机理。

关键词:三氟化钇;水热法;荧光
中图分类号:O614.33;O613.41 **文献标识码**:A **文章编号**:1001-4861(2010)02-0274-05

Hydrothermal Synthesis of YF_3 Microcrystals with Different Morphologies and Luminescent Properties of Eu^{3+}-Doped YF_3

WANG Miao SUN Tong-Ming SHI Yu-Jun*
(*School of Chemistry and Chemical Engineering, Nantong University, Nantong, Jiangsu* 226007)

Abstract: Hydrothermal approaches were used to synthesize microcrystals with YF_3 different morphologies (octahedron or ovals) from the reaction of $Y(NO_3)_3\cdot 6H_2O$ and K_2SiF_6 or KPF_6. The chemical composition was determined by X-ray photoelectron spectroscopy (XPS), no peak other than Y and F is observed. X-ray diffraction (XRD) patterns show that all as-prepared YF_3 products have the same orthorhombic structure. Scanning electron microscopy (SEM) and transmission electron microscopy (TEM) results indicate that the octahedral crystals of YF_3 have an edge length about 200 nm and the ovals are self-assembled by small nanocubes. The room temperature luminescent properties of Eu^{3+}-doped YF_3 crystals were also investigated. The possible formation mechanism is discussed.

Key words: trifluoride yttrium; hydrothermal; photoluminescence

Due to the high ionicity of the Y^{3+} to fluorine bond, YF_3 has very low vibrational energy and the quenching of the excited states YF_3. As a promising down/up conversion luminescent host matrix, YF_3 has recently attracted considerable attention in many research fields [1-4]. Since the chemical properties of inorganic nanocrystals usually depend on their sizes and shapes, a lot of efforts have been devoted to rationally control them, especially to the exploration of various simple and efficient approaches for preparing YF_3 materials. Among them, some relatively mild chemical procedures, such as hydrothermal pathways [2-9], precipitation [10-11], microwave routes [12] and microemulsion [13] have been developed to prepare YF_3 with different sizes and morphologies. So far, octahedron [3,9-10], hollow peanuts [7], spheres and bundles [10], quadrilateral and hexagonal nanocrystals [13-14] have been successfully obtained.

The most often used synthetic approaches employ

收稿日期:2009-08-20。收修改稿日期:2009-11-23。
江苏省高校自然科学基金(No.08KJB430012),南通市应用研究计划项目(No.K2008001),南通大学自然科学项目(No.09562),南通大学博士启动基金(No.08R07)资助项目。
*通讯联系人。E-mail:syj@ntu.edu.cn
第一作者:王 森,女,30 岁,博士,讲师;研究方向:功能纳米材料的制备及性质。

HF, NaF, NH_4F as fluoride source under a variety of reaction conditions. Recently, tetrafluroborate complexes have also been used as the fluoride source for the preparation of binary rare earth fluorides[7,15-19]. Our previous studies showed that, under hydrothermal conditions, YF_3 nanocrystals formed from $NaBF_4$, NH_4BF_4 or KBF_4 were self-assembled into hollow peanut-like structures[7]. Meanwhile, imidazolium ionic liquids (C_4mimBF_4 and C_4mimPF_6) (mim=methylimidazolium) were also employed to prepare YF_3 with controlled crystalline phases and novel morphologies [8,11-12]. Hydrothermal method has been used to prepare EuF_3[19], herein, we use two unique inorganic complex fluorides (K_2SiF_6 and KPF_6) as fluoride source to synthesize YF_3 under this facile and simple method. It is found that fluoride source and reaction time play crucial roles in the formation of different morphologies for final products.

1 Experimental

1.1 Preparation

Rare earth oxides Ln_2O_3(Ln=Y, Eu, 99.99%) were purchased from Shanghai Yue Long New Materials Corporation. The rare earth nitrate $Ln(NO_3)_3 \cdot 6H_2O$ was made by dissolving rare earth oxide in nitric acid(63%~65%) and then evaporating the solvent. All other chemicals used were analytical reagent grade and used as received without further purification. 1.0 mmol $Y(NO_3)_3 \cdot 6H_2O$ and 0.5 mmol K_2SiF_6(or KPF_6) were dissolved in 25 mL of distilled water in a plastic flask. After being stirred for 20 min at room temperature, the mixture was transferred into a 30 mL Teflon-lined stainless autoclave. After the autoclave was sealed and heated at 160 ℃ for a set time, it was naturally cooled to room temperature. A white solid was collected after centrifugation and then washed with distilled water and ethanol in an ultrasonic bath for several times. The solid was collected and dried at 70 ℃ for 3 h. At 160 ℃, 5mol% Eu-doped YF_3 samples were prepared during different reaction time.

1.2 Characterization

The crystalline phases of the products were analyzed by XRD on a Shimadzu XRD-6000 powder X-ray diffractometer (Cu $K\alpha$ radiation λ=0.154 18 nm), employing a scanning rate of 4.00°·min^{-1}, in the 2θ range from 10° to 80°. The operation voltage and current were maintained at 40 kV and 30 mA, respectively. The X-ray photoelectron spectra (XPS) were recorded on an ESCALAB MK Ⅱ X-ray photoelectron spectrometer, using Mg $K\alpha$ X-ray as the excitation source. The sizes and morphologies of the products were studied by a TECNAI F20S-TWIN transmission electron microscopy (TEM) and a JSM-6700F scanning electron microscopy (SEM). The luminescent spectra of the solid samples were recorded on HITACHI F-4500 spectrophotometer at room temperature.

2 Results and discussion

2.1 Structure characterization

The X-ray diffraction patterns of the as-obtained products are shown in Fig.1a. All the diffraction peaks can be readily indexed to orthorhombic crystalline phased YF_3. The positions of the peaks are in good agreement with values in the literature (PDF No.74-

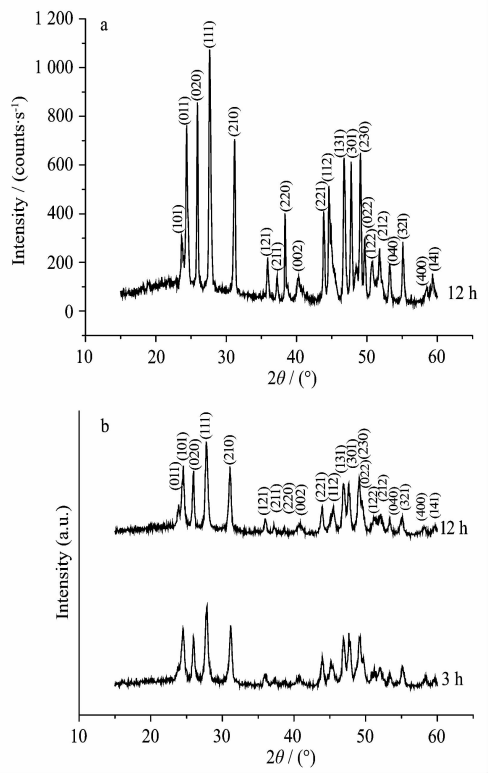

(a) K_2SiF_6(12 h); (b) KPF_6(3 h and 12h)

Fig.1　XRD patterns of the YF_3 from different fluoride sources

0911). No impurity peak is observed. XRD analyses show that products from KPF_6 ($n_{KPF_6}/n_{Y^{3+}}$=0.5) are both orthorhombic and changes of the reaction time do not affect the crystalline phase of the products(Fig.1b).

Fig.2 shows the XPS spectrum of the orthorhombic YF_3 from K_2SiF_6(12 h) and KPF_6(12 h), all peaks are assigned to Y and F except C and O peaks (probably from a source in the XPS chamber). The peak at about 685.1 and 159.7 eV corresponds to the F1*s* and Y3*d* binding energy, respectively. The results are in agreement with values in literature[7].

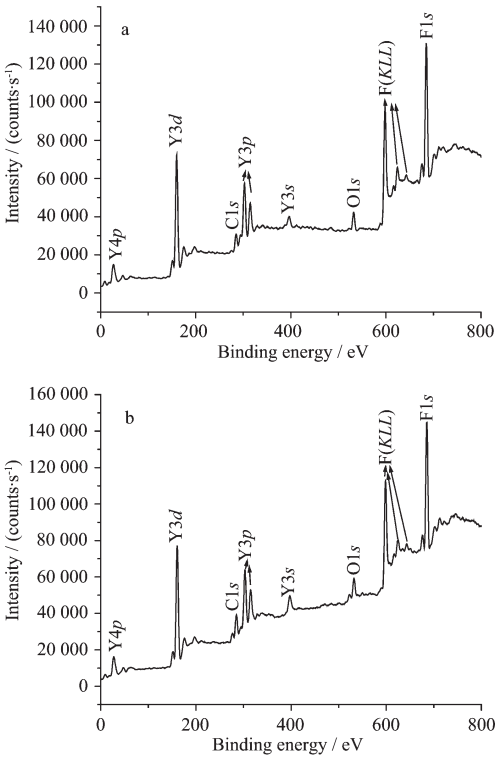

Fig.2 XPS spectrum of the YF_3 obtained from (a) K_2SiF_6 and (b) KPF_6 within 12 h

2.2 Morphology characterization

YF_3 solids are obtained from the reaction of $Y(NO_3)_3 \cdot 6H_2O$ with K_2SiF_6($n_{K_2SiF_6}/n_{Y^{3+}}$=0.5). Their TEM and SEM images(Fig.3a, b) show that they have microsized truncated octahedron shapes with the edge length of ca. 200 nm when the reaction time is 3 h. These unique shapes are similar to those in earlier reports [3,10]. After 6 h, the truncated parts of some octahedrons have grown completely into octahedron with clear borders (Fig.3c, d). Complete microsized octahedrons are formed after 9 h. Their SEM images are consistent with the TEM observation(Fig.3e, f). The most important observation is that the surfaces are not smooth and the octahedrons have layer-by-layer structures. Spheres with diameter of *ca.* 200 nm are prepared in a period of 12 h (Fig.3g). Controlled experiments have been carried out to investigate the effects of reaction parameters. The reaction temperature does not show a significant effect on the crystalline phases and morphologies. In addition, the molar ratio of the starting materials does not affect the crystalline phases and morphologies of the products, neither.

KPF_6, another inorganic complex fluoride, is also used as fluoride source to synthesize YF_3 by an identical procedure. TEM and SEM images of the products

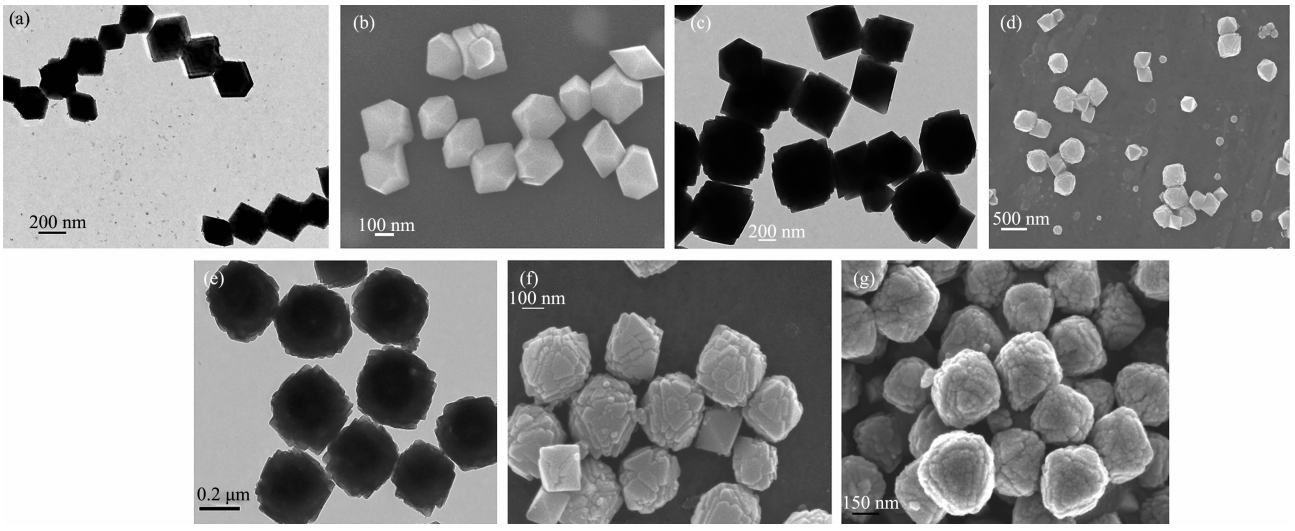

TEM images: a(3 h), c(6 h) and e(9 h); SEM images: b(3 h), d(6 h), f(9 h) and g(12 h)

Fig.3 TEM and SEM images of the YF_3 prepared from K_2SiF_6 in different periods of time

from KPF_6 are shown in Fig.4. The TEM image shows the YF_3 solid, obtained with 3 h, is small nanocubes with irregular shapes and their sizes are different from each other(Fig.4a). With the extension of reaction time (12 h), SEM(Fig.4b) and TEM(Fig.4c) images show the products become uniform ovals with length of ca. 300 nm and width of 200 nm, and the surfaces are rough. A magnified TEM image reveals that a single oval(Fig.4d) consists of small nanocubes, and the size of the nanocubes is identical to those in Fig.4a. These results suggest that the oval is formed by the self-assembly of small nanocubes during the reaction process. The morphological evolution of the product is similar to that using $NaBF_4$ as fluoride source[7].

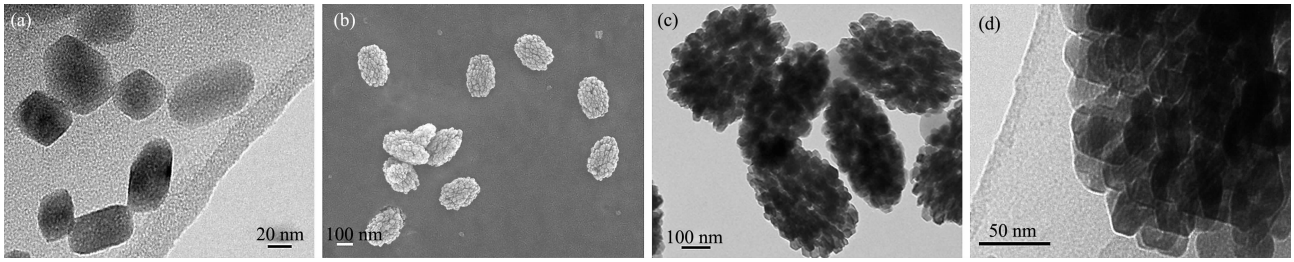

(a) TEM images 3 h; (b~d) SEM and TEM images, 12 h

Fig.4　TEM and SEM images of YF_3 obtained from KPF_6 during different periods of reaction time

2.3　The formation mechanism of YF_3

We previously used XBF_4(X=H, Na, NH_4 and K) as the fluoride source in the preparation of YF_3 and EuF_3 nanocrystals[7,16]. By varying the fluoride source, different morphological YF_3 can be controllably synthesized. Similar to BF_4^-, both SiF_6^{2-} and PF_6^- need to release F^- anions through a hydrolysis process, and F^- anions then react with Y^{3+} to form YF_3. The proposed reaction pathways are summarized as follows:

$$SiF_6^{2-}+3H_2O \longrightarrow 2F^-+H_2SiO_3+4HF \quad (\mathbf{1})$$

$$PF_6^-+4H_2O \longrightarrow F^-+H_3PO_4+5HF \quad (\mathbf{2})$$

$$Y^{3+}+3F^- \longrightarrow YF_3 \quad (\mathbf{3})$$

The Eqs(**1~3**) were reported earlier[8,19]. Our previous research also revealed that the cations of the simple binary fluoride source XF(X=K, H, NH_4, Na, Rb, or Cs) played an important role in the formation of EuF_3 nanocrystals with different morphologies[20]. In this study, it is obvious that the morphology of YF_3 can be controlled by varying the fluoride source. The positive ion in the fluoride source(KPF_6 or K_2SiF_6) is the same and the negative central ion is different. In our previous studies, in the case of KBF_4, a ring-like structure was formed by the self-assembly of the nanoblocks of EuF_3. However, only oval-like and blocks of EuF_3 formed with KPF_6 and K_2SiF_6, respectively [19]. Therefore, it is believed that the negative ions are responsible for the different morphologies of the as-prepared YF_3.

2.4　Luminescence properties

The room-temperature luminescent properties of 5mol% Eu-doped YF_3 samples, prepared from different conditions, are shown in Fig.5. When samples are excited at 395 nm, the corresponding emission peaks are observed at 592, 615, 651 and 692 nm. They originated from the transitions between the $^5D_0$ excited-state and the ^7F_J(J=1, 2, 3, 4) ground states of Eu^{3+} ion. Although the positions of the major peaks in the emission spectra are identical for these samples, but their emission intensity is different. This difference could be affected by their morphologies, dimensions and crystal structures.

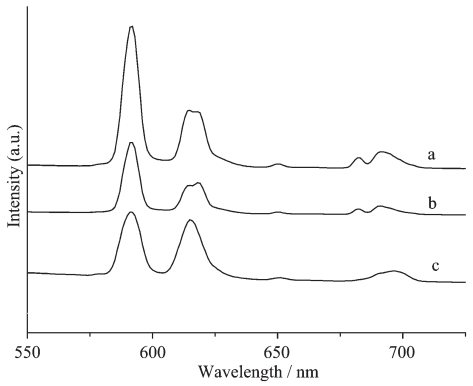

a: K_2SiF_6, 12 h; b: K_2SiF_6, 3 h; c: KPF_6, 12 h

Fig.5　Room temperature luminescence of the Eu-doped samples obtained from different conditions

3 Conclusion

Microsized octahedrons and ovals of YF_3 have been prepared by a hydrothermal route using K_2SiF_6 and KPF_6 as the fluoride sources. The time-dependent studies reveal that the oval-like YF_3 from KPF_6 undergoes a self-assembly process in the morphological evolution.

References:

[1] Iparraguirre I, Azkargorta J, Balda R, et al. *Opt. Mater.*, **2005**,**27**:1697-1703

[2] Yan R X, Li Y D. *Adv. Funct. Mater.*, **2005**,**15**:763-770

[3] Tao F, Wang Z J, Yao L Z, et al. *J. Phys. Chem. C*, **2007**, **111**:3241-3245

[4] Cui Y, Fan X P, Hong Z L, et al. *J. Nanosci. Nanotechnol.*, **2006**,**6**:830-836

[5] De G H, Qin W P, Zhang J S, et al. *J. Lumin.*, **2007**,**122-123**:128-130

[6] Wang X, Zhuang J, Peng Q, et al. *Nature*, **2005**,**437**:121-124

[7] Wang M, Huang Q L, Zhong H X, et al. *Cryst. Growth Des.*, **2007**,**7**:2106-2111

[8] Zhong H X, Hong J M, Cao X F, et al. *Mater. Res. Bull.*, **2009**,**44**:623-628

[9] Li G Y, Ni Y H, Hong J M, et al. *Cryst. Eng. Comm.*, **2008**, **10**:1681-1686

[10]Wang M, Huang Q L, Hong J M, et al. *Mater. Lett.*, **2007**, **61**:1960-1963

[11]Nunez N O, Ocana M. *Nanotech.*, **2007**,**18**:455606(7pp)

[12]Jacob D S, Bitton L, Grinblat J, et al. *Chem. Mater.*, **2006**, **18**:3162-3168

[13]Lemyre J L, Ritcey A M. *Chem. Mater.*, **2005**,**17**:3040-3043

[14]Yan Z G, Yan C H. *J. Mater. Chem.*, **2008**,**18**:5046-5059

[15]Miao Z J, Liu Z M, Ding K L, et al. *Nanotech.*, **2007**,**18**: 125605(5pp)

[16]Wang M, Huang Q L, Hong J M, et al. *Cryst. Growth Des.*, **2006**,**6**:1972-1974

[17]Zhu L, Meng J, Cao X Q. *Eur. J. Inorg. Chem.*, **2007**,**24**: 3863-3867

[18]WANG Miao(王 淼), SHI Yu-Jun(石玉军), JIANG Guo-Qing(江国庆). *Chinese J. Inorg. Chem.*(*Wuji Huaxue Xuebao*), **2009**,**25**:1785-1790

[19]Zhong H X, Wang M, Yang H L, et al. *Mater. Sci. Eng. B*, **2009**,**156**:62-67

[20]WANG Miao(王 淼), HUANG Qing-Li(黄庆利), CHEN Xue-Tai(陈学太), et al. *Chinese J. Inorg. Chem.*(*Wuji Huaxue Xuebao*), **2007**,**23**:1550-1554